Global prediction of δ_A and δ^2H-δ^{18}O evaporation slopes for lakes and soil water accounting for seasonality

J. J. Gibson,[1,2] S. J. Birks,[3,4] and T. W. D. Edwards[4]

Received 19 April 2007; revised 21 January 2008; accepted 7 February 2008; published 28 June 2008.

[1] Global trends in the δ^2H-δ^{18}O enrichment slope of continental lakes and shallow soil water undergoing natural evaporation are predicted on the basis of a steady state isotope balance model using basic monthly climate data (i.e., temperature and humidity), isotopes in precipitation data, and a simple equilibrium liquid-vapor model to estimate isotopes in atmospheric moisture. The approach, which demonstrates the extension of well-known conceptual models in stable isotope hydrology to the global scale, is intended to serve as a baseline reference for evaluating field-based isotope measurements of vapor, surface water, and soil water and as a diagnostic tool for more complex ecosystem models, including isotope-equipped climate models. Our simulations reproduce the observed local evaporation line slopes (4–5 range for lakes and 2–3 range for soil water) for South America, Africa, Australia, and Europe. A systematic increase in slopes (5–8 range for lakes) toward the high latitudes is also predicted for lakes and soil water in northern North America, Asia, and Antarctica illustrating a latitudinal (mainly seasonality-related) control on the evaporation signals that has not been widely reported. The over-riding control on the poleward steepening of the local evaporation lines is found to be the isotopic separation between evaporation-flux-weighted atmospheric moisture and annual precipitation, and to lesser extents temperature and humidity, all of which are influenced by enhanced seasonality in cold regions.

Citation: Gibson, J. J., S. J. Birks, and T. W. D. Edwards (2008), Global prediction of δ_A and δ^2H-δ^{18}O evaporation slopes for lakes and soil water accounting for seasonality, *Global Biogeochem. Cycles*, *22*, GB2031, doi:10.1029/2007GB002997.

1. Introduction

[2] Steady state isotope balance models have often been applied to estimate long-term average water balance conditions for lakes [*Dinçer*, 1968; *Gat*, 1995]. When these models are applied in climates with a pronounced seasonality in evaporation rates, especially in environments where ice cover is present, they frequently predict slopes that differ greatly from observations. In these environments the predicted evaporative enrichment slopes are commonly lower than observed, and have therefore resulted in poor agreement between oxygen-18 and deuterium estimates of water balance parameters, or have required use (or fitting) of kinetic fractionation factors that are not in agreement with the experimental studies [*Zuber*, 1983; *Gibson et al.*, 1993]. Here we present an extension to the well-known *Craig and Gordon* [1965] model of isotopic enrichment that accounts for the effects of seasonality. As the *Craig and Gordon* [1965] model is a universally applied model of the isotope exchange process during evaporation, we use it to derive reference values for evaluating sensitivity of the process to local conditions. Application of this model on a global scale provides a baseline reference for evaluating isotope-equipped models as well as providing insight into the potential labeling of atmospheric moisture sources.

[3] One of the primary outcomes of this analysis is an awareness of the degree to which seasonality can influence evaporative enrichment, one of the most robust and distinctively labeled processes in the water cycle. Overall, we establish that for nonseasonal systems where precipitation-vapor equilibrium is assumed, it is expected that slope of the local evaporation line (LEL) for lakes is typically less than 5, and less than 3 for the upper soil layers. However, in climates with a pronounced seasonality in evaporation rates, the slope of the LEL depends on the open water season temperature and relative humidity and on the isotopic separation between the annual precipitation (δ_P) and the evaporation-flux-weighted atmospheric moisture ($\delta_A^{\text{evap.fw}}$), as shown in Figure 1.

2. Theory

[4] Stable isotope tracing of evaporation and related ecosystem processes at the local, regional, and global scale requires baseline information on isotopic signatures of precipitation and atmospheric moisture, as well as general

[1]Alberta Research Council, Victoria, British Columbia, Canada.
[2]Department of Geography, University of Victoria, Victoria, British Columbia, Canada.
[3]Alberta Research Council, Calgary, Alberta, Canada.
[4]Department of Earth and Environmental Sciences, University of Waterloo, Waterloo, Ontario, Canada.

0886-6236/08/2007GB002997

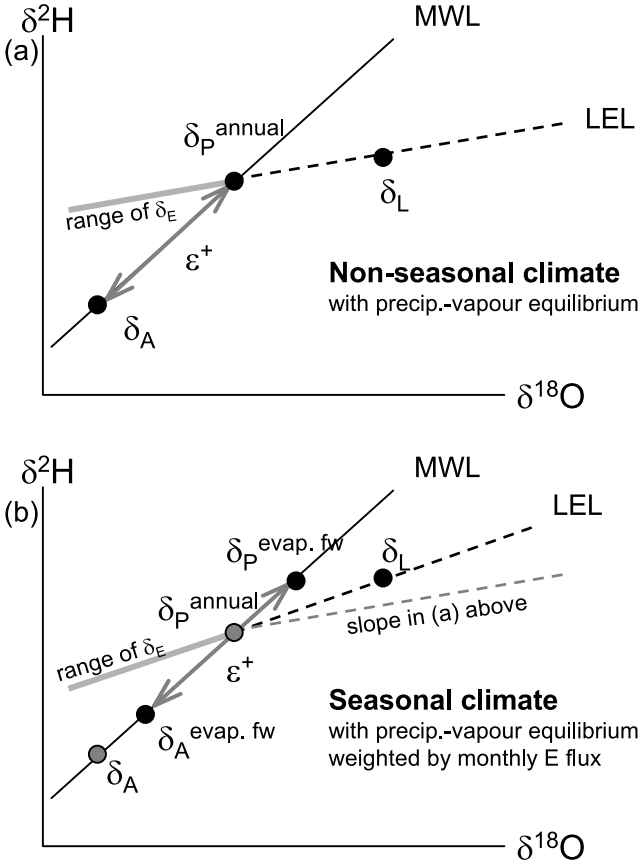

Figure 1. Plots of δ^2H-δ^{18}O showing the conceptual model of evaporative isotope enrichment (a) for a nonseasonal climate with constant monthly evaporation rate, assuming precipitation-vapor isotopic equilibrium, and (b) for a seasonal climate with variable monthly evaporation rate, assuming precipitation is evaporation-flux-weighted. Note that the isotopic separation between the effective long-term liquid and vapor is less than equilibrium in Figure 1b because of the seasonality effect (i.e., $\delta_P^{\text{annual}} - \delta_A^{\text{evap.fw}} < \varepsilon^+$). Note that ε^+ is evaluated at annual and monthly flux-weighted temperature for Figures 1a and 1b, respectively.

physioclimatic factors such as relative humidity and temperature that control the boundary layer structure and degree of equilibrium and kinetic isotopic fractionation [see *Gonfiantini*, 1986]. While biotically mediated vapor loss (transpiration) is generally nonfractionating [*Gat*, 1996], evaporation from open water bodies or soils produces heavy-isotope enrichment in the residual liquid and leads to a characteristic offset from the meteoric water line (MWL) in δ^2H-δ^{18}O space (Figure 1). (Isotopic ratios are reported in standard "δ" notation as deviations in per mil (‰) from Vienna Standard Mean Ocean Water (SMOW), such that $\delta_{\text{SAMPLE}} = 1000\,((R_{\text{SAMPLE}}/R_{\text{VSMOW}}) - 1)$, where R is $^{18}O/^{16}O$ or $^{2}H/^{1}H$.) Whereas precipitation typically clusters along the so-called Global Meteoric Water Line of *Craig* [1961] given by $\delta^2\text{H} = 8\delta^{18}O + 10$ and hence along a slope close to 8, the stronger kinetic effects for ^{18}O relative to ^{2}H lead to evaporative enrichment of residual liquid along lines of lower slope. Deep groundwaters are expected to retain much of the isotopic signature of precipitation unless selective or episodic recharge of evaporatively enriched soil water is a locally important process in the hydrological cycle.

[5] The isotopic composition of precipitation is controlled by a number of factors and processes, including (1) meteorological conditions (relative humidity, sea surface temperature and wind regime) controlling evaporation of water from the ocean, (2) rainout mechanisms, which influence the fraction of precipitable water, (3) second-order kinetic effects such as snow formation or evaporation below cloud base, (4) mixing of air masses from different oceanic source regions [*Araguás-Araguás et al.*, 2000], and (5) admixture of recycled water from evapotranspiration over the continents [*Gat*, 2000].

[6] A simplified version of the Craig-Gordon model neglecting resistance to mixing in the liquid phase is commonly employed to describe relative changes in the isotopic composition of the evaporating flux (δ_E) and the residual liquid (δ_L) as water undergoes evaporation [*Gonfiantini*, 1986]:

$$\delta_E = \frac{1}{1-h+\varepsilon_K}\left(\frac{\delta_L - \varepsilon^+}{\alpha^+} - h\delta_A - \varepsilon_K\right) \tag{1}$$

where h is the relative humidity; α^+ is the liquid-vapor equilibrium isotopic fractionation, estimated from empirical relations derived by *Horita and Wesolowski* [1994] (for δ^2H, $1000\ \ln\alpha^+ = 1158.8(T^3/10^9) - 1620.1(T^2/10^6) + 794.84(T/10^3) - 161.04 + 2.9992(10^9/T^3)$, and for δ^{18}O, $1000\ \ln\alpha^+ = -7.685 + 6.7123(10^3/T) - 1.6664(10^6/T^2) + 0.35041(10^9/T^3)$); ε^+ is the equilibrium isotopic separation between liquid and vapor, calculated as $\varepsilon^+ = (\alpha^+ - 1)$; ε_K is the equivalent kinetic isotopic separation based on wind tunnel experiments [e.g., *Vogt*, 1976; *Merlivat*, 1978; see also *Gonfiantini*, 1986], as discussed further below; and δ_A is the isotopic composition of ambient atmospheric vapor. Note that equation (1) is formulated for h, δ and ε values in decimal notation.

[7] Isotopic measurements of local water vapor at ground level reveals that in most cases equilibrium is maintained between vapor and precipitation over the continents [*Araguás-Araguás et al.*, 2000], rain being the most common form of precipitation during the evaporation season. Values for the isotopic composition of δ_A have thus often been estimated on the basis of assumed isotopic equilibrium between atmospheric moisture and precipitation [*Rozanski et al.*, 2001; *Gibson et al.*, 1993], although this hypothesis remains to be rigorously tested. *Gat et al.* [1994], *Gat and Matsui* [1991] and others have shown that isotopic composition of precipitation inherently reflects recycled moisture admixtures, including biospheric water and evaporate. Estimates of the mean annual δ_A in arid climates are more difficult to determine because of the irregular distribution of precipitation events over the course of a year.

[8] A key diagnostic variable of mass conservation for both hydrogen and oxygen isotopes during the evaporation process is the capacity of a model to predict the observed

slopes of the local evaporation lines (LELs) for soil and open water in δ^2H-δ^{18}O space. For ideal reservoirs (either a lake or soil water pool fed by local precipitation), the slope of the LEL (S_{LEL}) predicted by the Craig-Gordon model is

$$S_{LEL} = \frac{\left[\frac{h(\delta_A - \delta_P) + (1+\delta_P)(\varepsilon_K + \varepsilon^+/\alpha^+)}{h - \varepsilon_K - \varepsilon^+/\alpha^+}\right]_2}{\left[\frac{h(\delta_A - \delta_P) + (1+\delta_P)(\varepsilon_K + \varepsilon^+/\alpha^+)}{h - \varepsilon_K - \varepsilon^+/\alpha^+}\right]_{18}} \quad (2)$$

where δ_A and δ_P are the isotopic compositions of atmospheric moisture and precipitation, respectively (again formulated for h, δ and ε values in decimal notation). This is sometimes termed the equilibrium evaporation slope, which applies to evaporation of local precipitation [see *Gat and Bowser*, 1991], but is distinguished from nonequilibrium evaporation slopes, which describe evaporation of allochthonous water sources, i.e., waters introduced by long-distance river transport, regional groundwater flow, or artificial diversions. Local evaporation lines (LELs) have been widely reported from field studies of water bodies [e.g., *Dinçer*, 1968; *Zuber*, 1983; *Gibson*, 2002; *Gibson et al.*, 1993, 2005] and soil water [e.g., *Barnes and Allison*, 1988; *Allison et al.*, 1983]. In general, soil water LELs have been reported as having lower slopes than open water LELs, attributed to vapor transport through the stagnant, diffusion-dominated soil matrix. Turbulence associated with evaporation from open water surfaces under typical wind conditions reduces kinetic fractionation by half [*Gat*, 1996].

[9] Observed LEL slopes for water bodies typically range from 4.0 to 5.5 for most regions, although studies in Arctic Canada have suggested a systematic poleward steepening of the local evaporation lines [see *Gibson et al.*, 2005], while soil water LEL slopes are generally less than 3.

[10] Previous studies have applied equation (2) to predict LEL conditions relevant to local study sites, but the approach has not been previously applied at a regional or global scale largely because of lack of available information on the isotopic composition of atmospheric moisture.

2.1. Method

[11] To develop a better understanding of potential regional variations in slopes that influence labeling of evaporated water, we apply equation (1) to station data on a global scale, incorporating evaporation-flux-weighting as a means to account for seasonality. In this analysis, precipitation is used as a systematic proxy for the isotopic composition of atmospheric moisture. Values for δ_A were determined using the precipitation-equilibrium assumption:

$$\delta_A = (\delta_P - \varepsilon^+)/\alpha^+ \quad (3)$$

[12] Because evaporation (E) occurs under seasonally variable environmental conditions, the exchange terms δ_A, ε^+, ε_K, and h in equation (2) were evaluated on a monthly time step and evaporation-flux-weighted to simulate the expected annual δ^2H-δ^{18}O trajectories. At the same time the annual precipitation δ_P values were amount-weighted from monthly data as these are expected to mimic the annual average source water to lakes and soil water. The analysis was conducted globally for terrestrial surfaces to derive annual δ_A climatologies for both δ^2H and δ^{18}O. For each tracer the ε^+ values were derived using the equations of *Horita and Wesolowski* [1994], as noted above, and ε_K values were based on $\varepsilon_K = nC_K^o\ \theta\ (1 - h)$ where C_K^o is 25.0‰ and 28.6‰ for deuterium and oxygen-18, respectively, $n = 1/2$ for open water bodies and $n = 1$ for soil water, and $\theta = (1 - h')/(1 - h)$ is an advection term to account for the potential influence of humidity buildup, h' being the adjusted humidity of the downwind atmosphere following admixture of evaporating moisture over the surface, often set to $\theta \approx 1$ for small water bodies [*Vogt*, 1976; *Gonfiantini; 1986*; *Gat*, 1996].

[13] The global isotope climatology used here is based on station data used to assemble a gridded precipitation data set by *Birks et al.* [2002], but also includes additional station data from the Siberian Network for Isotopes in Precipitation (SNIP) (Figure 2a) [*Kurita et al.*, 2004]. The NCEP/NCAR reanalysis data set [*Kalnay et al.*, 1996] was used to obtain monthly climatologies of T, h and E for each of the stations used in this analysis. These values were extracted from 2.5° × 2.5° grid cells and consequently may not be representative of conditions at point locations within each grid, particularly in areas of high relief and for grid cells adjacent to oceans. As a sensitivity test, S_{LEL} values were calculated using equation (2) and a variety of different estimates for T, h and E so that comparisons between S_{LEL} values obtained using different values for each of these parameters could be made. Included in our comparisons were runs made with different estimates of T (surface, 2m and 1000 mbar), h (calculated using temperature and specific humidity, and 1000 mbar relative humidity), and E (potential evaporation rate and latent heat flux, which are available directly as reanalysis products, as well as calculated potential E, based on T and h). The calculated S_{LEL} values using these different combinations of parameters retained the general relationship between S_{LEL} and latitude, as well as the range of S_{LEL} values, regardless of which of the estimates of T, h and E were used, but differed in the number of outliers (unrealistic $S_{\mathrm{LEL}} < 0$). Closer inspection of outliers revealed that they were primarily high-elevation stations, where all of our reanalysis-based h estimates were significantly larger than station-measured climate normals. Six such stations were removed from the data set. The S_{LEL} estimates we present here were calculated using 2m temperatures and 1000 mbar h. Note that no additional ice freeze-over or break-up masks are applied to depict the occurrence of the open water period, although precise timing of these events might be an important modifier of environmental conditions during individual spring/fall months in high-latitude or high-altitude systems. Because these months also tend to have lower evaporation rates (at least for small lakes) it was assumed for the purposes of this analysis that the annual flux-weighting would not be significantly affected by disregarding the intramonth timing of these processes. To gain a better appreciation of the spatial variations in the estimates of S_{LEL}, δ_{A} and δ_{P} the values determined for each of the stations were interpolated onto a 2.5° × 2.5° grid using a Cressman objective analysis, a spheres of influence

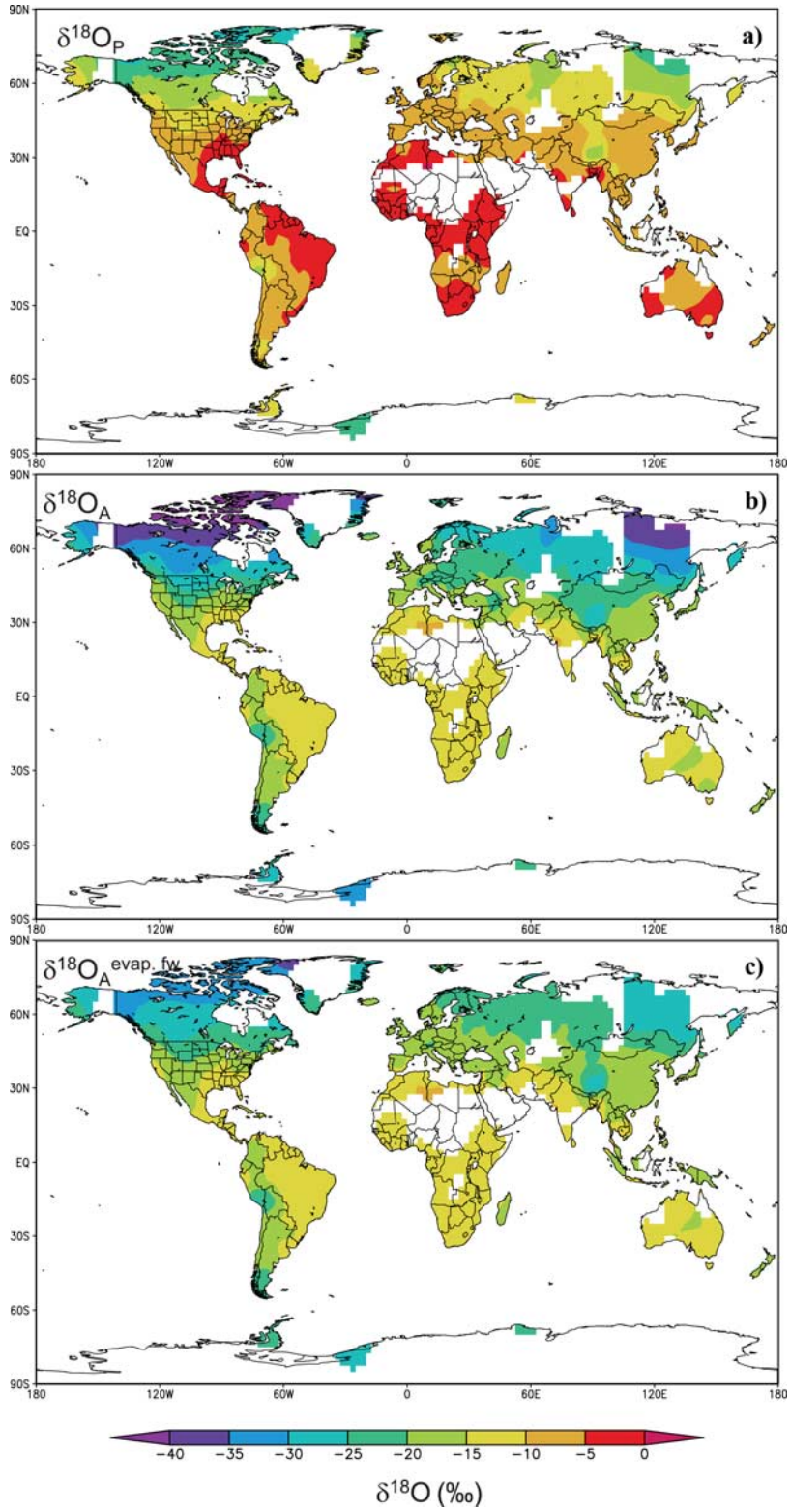

Figure 2. Plots of $\delta^{18}O$ in the following: (a) mean annual amount-weighted precipitation based on monthly data of *Birks et al.* [2002] with additional data from Siberian Network for Isotopes in Precipitation (SNIP) [*Kurita et al.*, 2004], (b) mean annual atmospheric moisture composition assuming liquid-vapor equilibrium with annual precipitation above, and (c) evaporation-flux-weighted atmospheric moisture assuming liquid-vapor equilibrium.

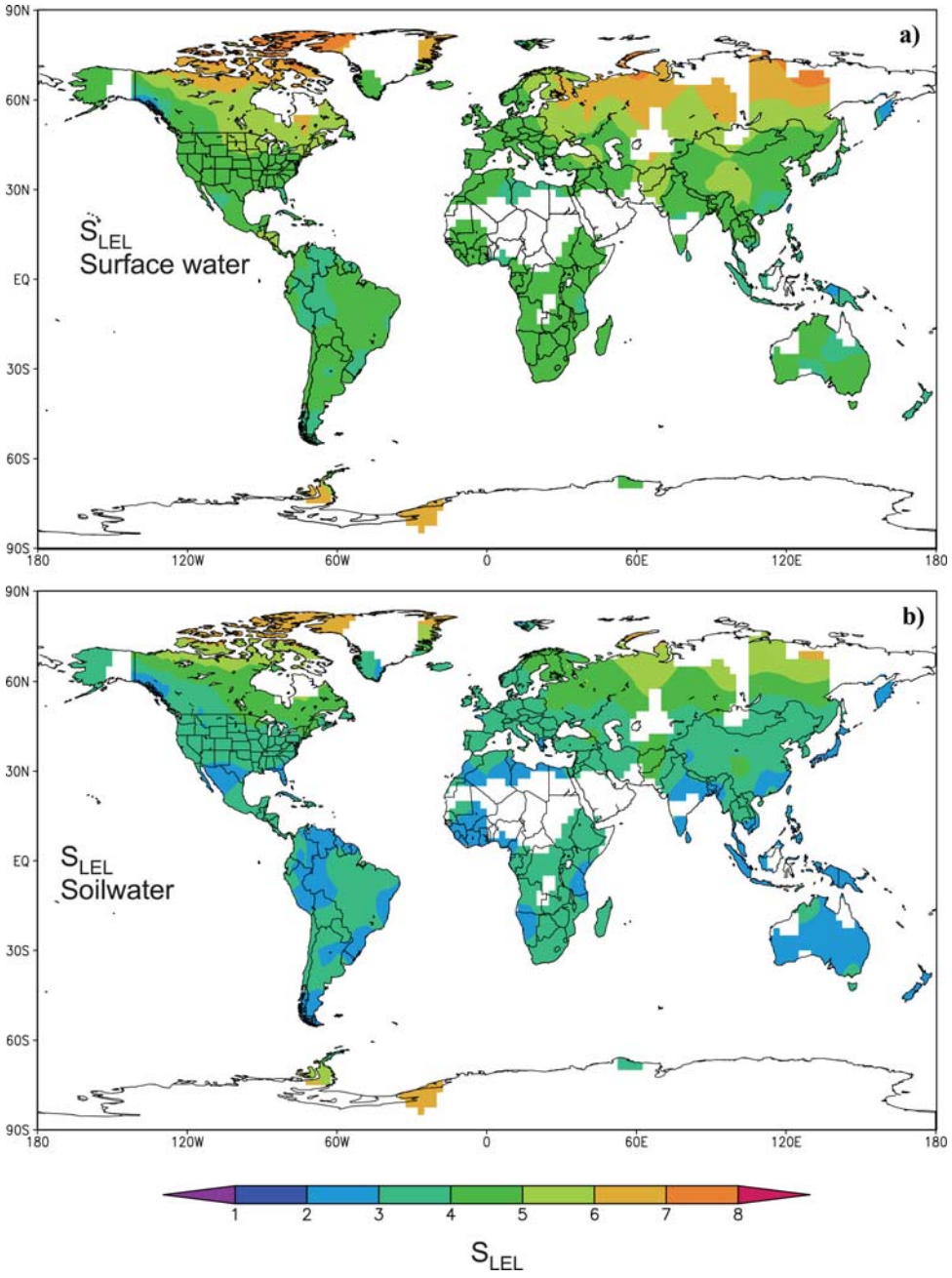

Figure 3. Modeled slopes of equilibrium local evaporation lines calculated for (a) surface waters and (b) soil water.

method developed for interpolating meteoric data [*Cressman*, 1959].

2.2. Results

[14] Maps illustrating $\delta^{18}O$ results for atmospheric moisture include amount-weighted mean annual $\delta^{18}O$ of precipitation (Figure 2a), the atmospheric moisture $\delta^{18}O$ assuming equilibrium with precipitation without monthly evaporation-flux-weighting (Figure 2b), and finally, the $\delta^{18}O$ of atmospheric moisture with monthly evaporation-flux-weighting (Figure 2c). Maps illustrating the predicted slope of evaporation lines include ideal precipitation-fed lakes under turbulent rough surface conditions (Figure 3a), precipitation-fed soil water with purely diffusive water transport (Figure 3b). Intermediate slope values would be expected for the situation of smooth open water conditions, not common in most natural system (not shown). The predicted slope values for each of the stations used in the maps in Figure 3 are presented in Figures 4a–4c. The effect of flux-weighting becomes apparent in Figure 4a where slopes were calculated using equation (2) and annual average values of δ_A, ε^+, ε_K and h, instead of values representative of the open water

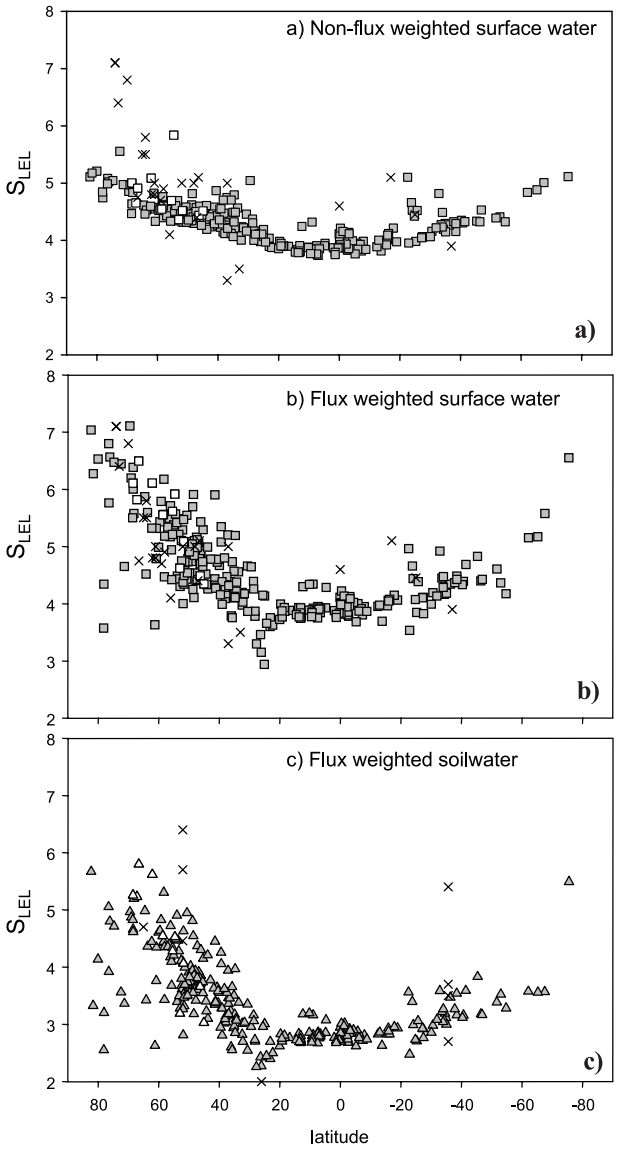

Figure 4. Slopes calculated using equation (2) for each of the Global Network for Isotopes in Precipitation (GNIP) (solid symbols) and SNIP (open symbols) stations, compared to observations compiled from Tables 1a and 1b (cross symbols). In Figure 4a, average annual values of δ_A, ε^+, ε_K, and h are used in the calculations, producing a fairly uniform predicted slope regardless of latitude. When the same calculations are performed using evaporation-flux-weighted values, a pronounced steepening of the predicted S_{LEL} for (b) lakes and (c) soil water becomes apparent.

season. When these parameters are flux-weighted (Figures 4b and 4c) regional differences in slopes become apparent. Evaporation-flux-weighting the variables in equation (2) gives estimates of δ_A, ε^+, ε_K, and h that reflect the values most representative of periods when lakes undergo evaporation. A comparison with available observations of the evaporation slopes reported elsewhere is given in Tables 1a and 1b and shown for comparison in Figure 4. Note that the poleward steepening in predicted slopes in the flux-weighted scenario appears to be a better match to the observations. It is important to note also that this poleward steepening cannot be attributed to uncertainties in estimating relative humidity at high latitudes, which can occur because of instrumental bias at very low temperatures [*New et al.*, 1999], since overestimation of h in these areas would result in a decrease in the calculated slopes at high latitudes, rather than this increasing trend.

2.3. Discussion

[15] While the use of evaporation flux-weighting for $\delta_A - \delta_P$ separation remains to be rigorously tested, the new conceptual model is capable of simulating the observed steepening of the LELs at higher latitudes while using a consistent set of exchange parameters. Lower slopes predicted by the original conceptual model at high latitudes (e.g., Figure 4a) are evidently due to improper (or lack of) weighting for the $\delta_A - \delta_P$ separation, which does not account for the fact that evaporation and isotope exchange does not occur during periods of ice cover or that the process is seasonally variable. The effects of evaporation-flux-weighting on the $\delta_A - \delta_P$ separation is clearly illustrated in δ^2H-δ^{18}O space (Figure 5) where accounting for the timing of the evaporation flux during the season results in a compression of the δ_A values that surface and soil waters equilibrate with over the active period (Figure 5c) when compared with the annual average δ_A values encountered over the entire year (Figure 5b). Regions where flux-weighting has the greatest influence are those with the greatest seasonality, as evident in Figures 6a and 6b.

[16] An interesting point that is particularly relevant to paleoclimate studies is that temporal changes in seasonality may have altered the slope of the local evaporation in the past. Application of dual ^{18}O and deuterium tracers to lake sediment archives may therefore be able to trace changes in paleoslope of the evaporation line and provide a basis for examining past seasonality signals. For modern water balance applications, the use of nonweighted atmospheric moisture values and standard exchange parameters can result in substantial errors in computed long-term values for evaporation-to-inflow ratios, particularly for strongly seasonal climates where errors may be as high as 50% for low-throughflow/high-evaporation lakes.

[17] On the basis of our model of the effects of seasonality on the isotopic labeling of evaporation, we would expect the slope of local evaporation lines to vary globally with lower values near the equator and higher values at high latitudes and altitudes, providing a readily testable hypothesis by spatial surveys of stable isotopes in lake water. Our model predicts lakes in midlatitude regions to have slopes ranging from 4 to 5, which is consistent with the ranges reported for lakes in most regions of the world (Tables 1a and 1b; see also Figure 4). The only high-latitude data available are for the Canadian Arctic and Siberia where the reported δ^{18}O and δ^2H values result in LELs with slopes > 5 are also predicted by our modeling (Table 1a). This trend has already been noted in northern Canada [*Gibson et al.*, 2005]. There are relatively fewer soil water δ^{18}O and δ^2H data available to compare with our modeled estimates

Table 1a. Summary of Published S_{LEL} Values for Surface Waters

Location (Surface Water)	Observed $S_{LELsurface\ water}$	Reference
North America		
>60	4.8–7.1	[*Gibson et al.*, 2005]
<60	4.1–4.7	[*Gibson et al.*, 2005]
Greenland		
Close to icesheet	3.9	
Coastal	4.9–5.6	[*Leng and Anderson*, 2003]
Europe		
Germany	5	[*von Grafenstein*, 2002]
Austria	4.4	[*Yehdegho et al.*, 1997]
Switzerland	5.1	[*Teranes and McKenzie*, 2001]
Poland	5	[*Zuber*, 1983]
Scandinavia		
Southern Sweden	4.9	[*Hammarlund et al.*, 2003]
Siberia		
Taimyr Peninsula	6.8	[*Wolfe and Edwards*, 1997]
Turkey		
Egridir and Beysehir	5	[*Dinçer*, 1968]
South America		
Andes	5.1	[*Wolfe et al.*, 2001]
Africa		
Sahel Lakes	4.6	[*Fontes and Gonfiantini*, 1967]
Mt. Menka	4.6	[*Rietti-Shati et al.*, 2000]
Australia		
Western Queensland	4.3–4.6	[*Hamilton et al.*, 2005]
South Australia	3.9	[*Turner et al.*, 1984]
Asia		
Western Tibet	3.5	[*Fontes et al.*, 1996]
Western China	3.3	[*Yang et al.*, 1995] saline

(Table 1b). With the exception of fairly high soil water slopes reported by *Darling and Bath* [1988] the slopes found for soil water are systematically lower than those reported for surface waters as our model predicts.

[18] The reason for the poleward steepening of the predicted LEL slopes becomes evident with closer examination of equation (2). The humidity dependence of S_{LEL} varies with the seasonality of the system. Seasonality results in compression of the apparent separation between δ_A and δ_P to values much less than ε^+ (shown schematically in Figure 1). In nonseasonal climates evaporation from water bodies is distributed equally over the entire year. This is in stark contrast to highly seasonal climates which have a strong bias in the timing of evaporation. In extreme cases such as at very high latitudes, frozen conditions can effectively isolate water bodies from the atmosphere for greater than 10 months of the year. Flux-weighting the transfer terms by evaporation effectively accounts for the greater importance of meteorological conditions during periods when the majority of evaporation is occurring, instead of relying on annual averages. In seasonal climates the weighted mean annual composition of precipitation (δ_P) will still likely be the starting point for evaporation for lakes and soil water, however, the atmospheric moisture (δ_A) to which the evaporating water body is exposed will be representative of the evaporation-flux- weighted δ_A (see Figure 2). In addition, the evaporation will occur under relative humidity and temperature conditions representative of the evaporative season, not the entire year (Figure 7).

3. Implications

[19] Quantifying the offset of lakes and rivers from the MWL along LELs has been used within the context of an

Table 1b. Summary of Published S_{LEL} Values for Soil Waters

Location (Soil Water)	Observed $S_{LELsoil\ water}$	Reference
North America		
NWT	4.7	based on data from *Stewart* [1994]
Saskatchewan	4.46	[*Maulé et al.*, 1994]
Europe		
UK	5.7 to 6.4	[*Darling and Bath*, 1988]
Africa		
Sahara	2	[*Dinçer et al.*, 1974]
Australia		
Western Queensland	3.7 to 5.4	[*Allison and Hughes*, 1983]
South Australia	2.7 to 3.5	[*Allison et al.*, 1983]

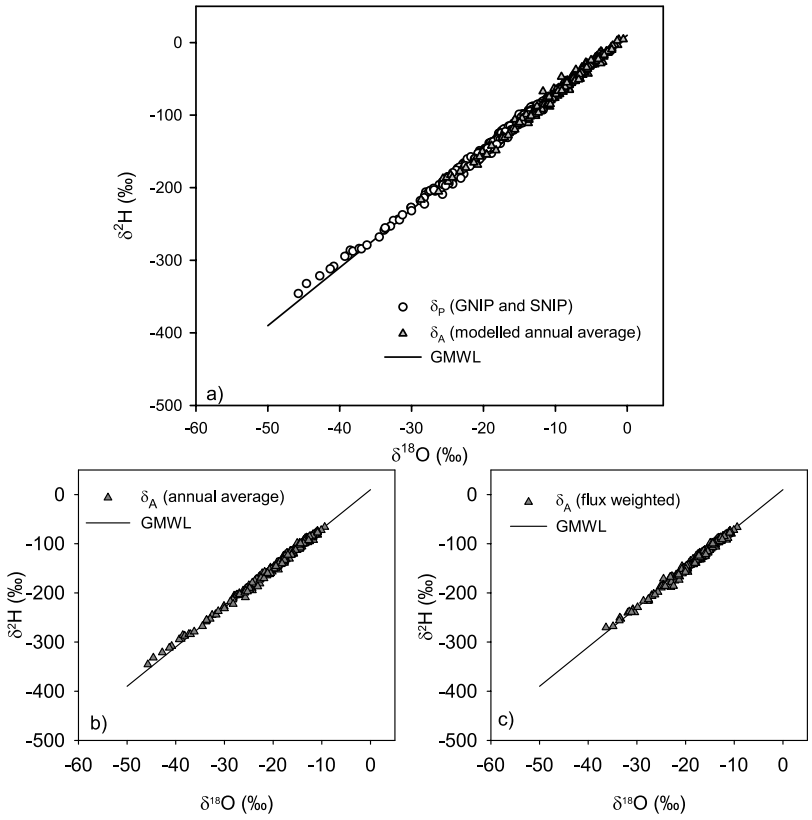

Figure 5. (a) The δ^2H-δ^{18}O relationship for precipitation (δ_P) for all stations contained in the GNIP and SNIP data sets plotted with the modeled atmospheric water vapor (δ_A) and the Global Meteoric Water Line (GMWL). Examining the calculated δ_A values without (b) and with (c) evaporation flux-weighting illustrates the importance of seasonality in determining the ambient atmospheric conditions when surface water evaporates.

isotope-mass balance analysis to partition water budget components, whereby fractionating losses (e.g., open water evaporation) are distinguished from nonfractionating losses (e.g., liquid outflow or transpiration). The dual tracer approach, using both ^{2}H and ^{18}O has generally been most successful in this application because of the ability to positively identify open water evaporation effects in the residual liquid as described above, but also for its ability to constrain errors, or unknown water budget components such as the isotope composition of atmospheric moisture, or kinetic fractionation factors. An evolution of practical approaches has been demonstrated over time [see *Gibson et al.*, 2005]. For a simple open water body with liquid outflow and evaporation, the fraction of evaporation losses can be estimated for each tracer from the isotopic offset in the residual liquid as

$$E/I = (\delta_P - \delta_L)/(\delta_E - \delta_L) \quad (4)$$

where δ_P, δ_L and δ_E are the isotopic compositions of precipitation, lake water and evaporate, respectively, and I is the isotopic composition of local precipitation-derived inflow. Because of practical difficulties in direct sampling of δ_E, this value is commonly characterized indirectly on the basis of knowledge of the boundary layer conditions using the Craig-Gordon model (equation (1)). For systems in which evaporation and transpiration are both significant, outflow gauging records can be used to partition the nonevaporated fraction between transpiration losses and liquid outflows [see *Gibson et al.*, 2005].

[20] The effect of seasonality on the slope of local evaporation lines has implications for the partitioning of evaporation and transpiration using water isotope tracers. A variety of conceptual isotopic labeling scenarios are given for an idealized evapotranspiring system comprising lakes or storage reservoirs and vegetated transpiring land surfaces in various climatic situations (Figures 8a–8c). As shown, the seasonality effect has little impact on the predicted LEL slopes at low latitudes (Figure 8a), with both the Craig-Gordon model and our seasonal model predicting slopes of about 4. Lakes in these regions are typically close to isotopic steady state, so that δ_E tends to be similar to δ_P. While liquid water partitioning is therefore likely to be successful, the vapor fluxes δ_E and δ_T are likely to be poorly distinguished with both being approximately equal to the mean annual δ_P composition, resulting in a situation where one should expect little potential for vapor partitioning using isotope tracers on an annual timescale. Short-term

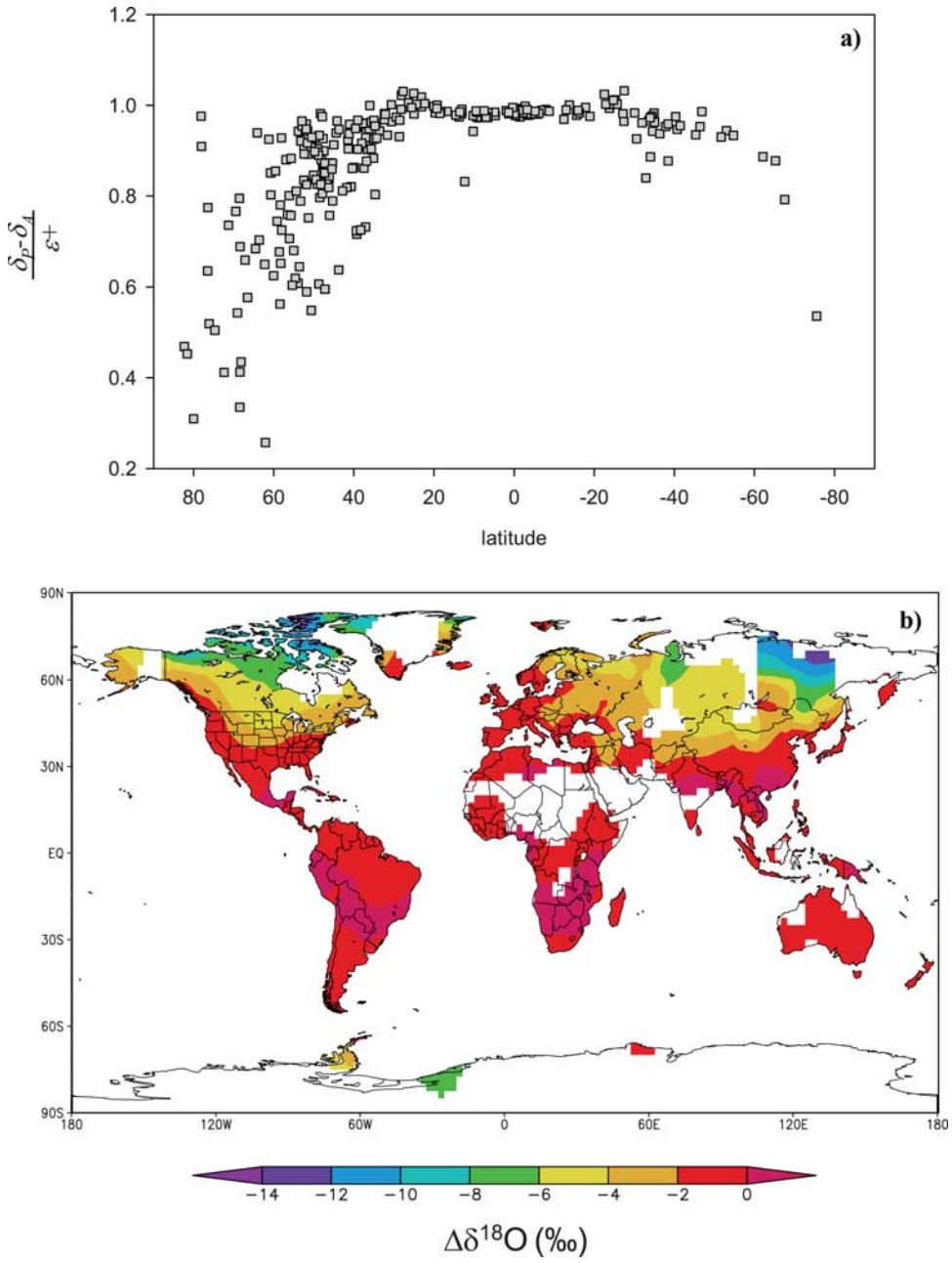

Figure 6. The regions where evaporation-flux-weighting has the largest influence become apparent in (a) the latitudinal distribution of $(\delta_P - \delta_A)/\varepsilon^+$ and in (b) the difference between the average annual δ_A of water vapor $\delta^{18}O$ and the evaporation-flux-weighted average water vapor ($\delta_A^{evap.\ fw}$). Note that ε^+ in Figure 6a is evaluated using annual temperature.

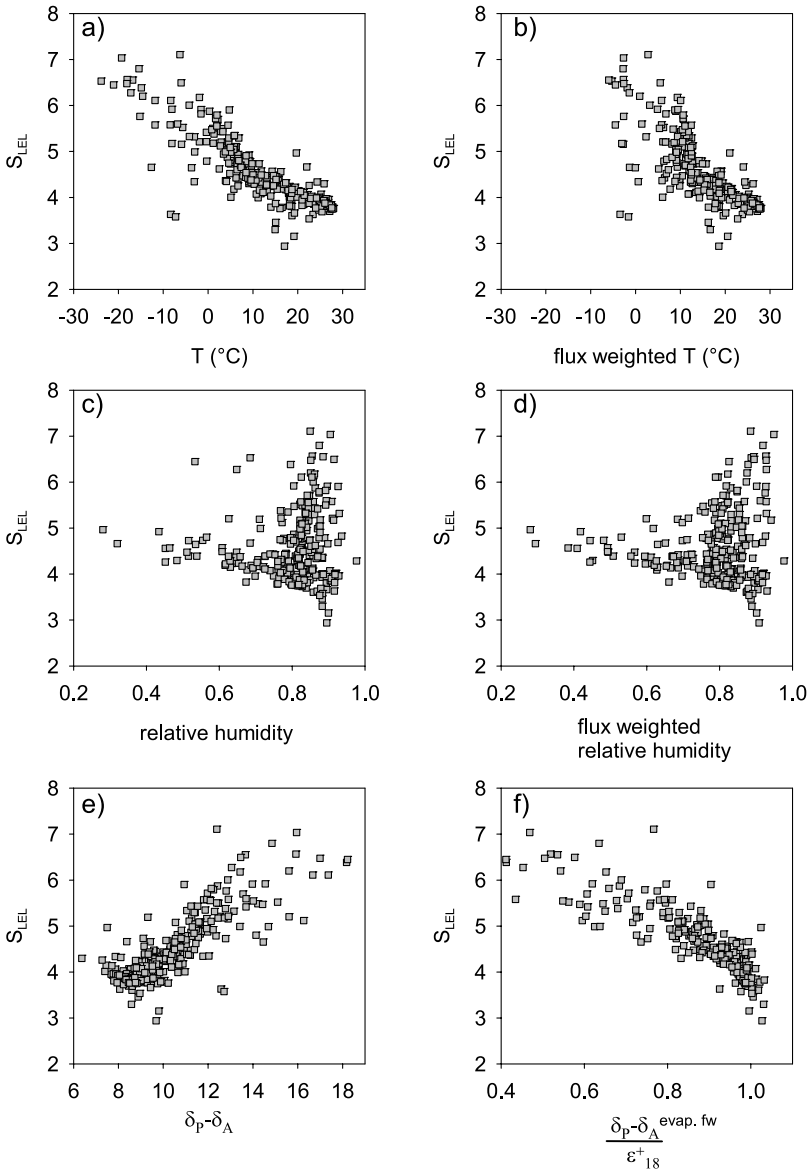

Figure 7. The effects of evaporation flux-weighting are evident in comparisons of predicted S_{LEL} and temperature (a–b), relative humidity (c–d), and for ^{18}O, the separation between δ_P and δ_A (e) and the evaporation flux-weighted separation normalized to the predicted equilibrium separation for ^{18}O (f). Evaporation flux-weighting results in the flux-weighted temperatures being significantly higher than the seasonal averages. In regions having high S_{LEL} the flux-weighted relative humidities are higher than the seasonal averages. The separation between weighted mean annual precipitation δ_P and the equilibrium predicted δ_A is greatest in regions with the highest S_{LEL} (Figure 7e). The greatest deviation between the flux-weighted separation and predicted separation also occurs in regions with the highest slopes (Figure 7f). Note that $\varepsilon_{18}{}^{+}$ is an estimate for ^{18}O based on annual temperature.

variations may still produce significant temporal offsets, but on the long term these differences are likely to diminish.

[21] The situation changes in midlatitude regions where lakes are less likely to reach isotopic steady state (Figure 8b). Our seasonal conceptual model predicts that slopes of local evaporation lines in these settings should be slightly steeper (5–6) than predicted by the Craig-Gordon model (~4). In these areas the δ_E produced from evaporating surface waters will be isotopically distinct from precipitation and transpiration because the slopes of the LELs should be sufficiently different from the local meteoric water line if the lakes are not at isotopic steady state. Transpiration in these settings will resemble weighted mean annual precipitation and the isotopic difference between δ_E and δ_T suggests there should be potential for partitioning these fluxes using isotope tracers both in the residual liquid and in the vapor phase.

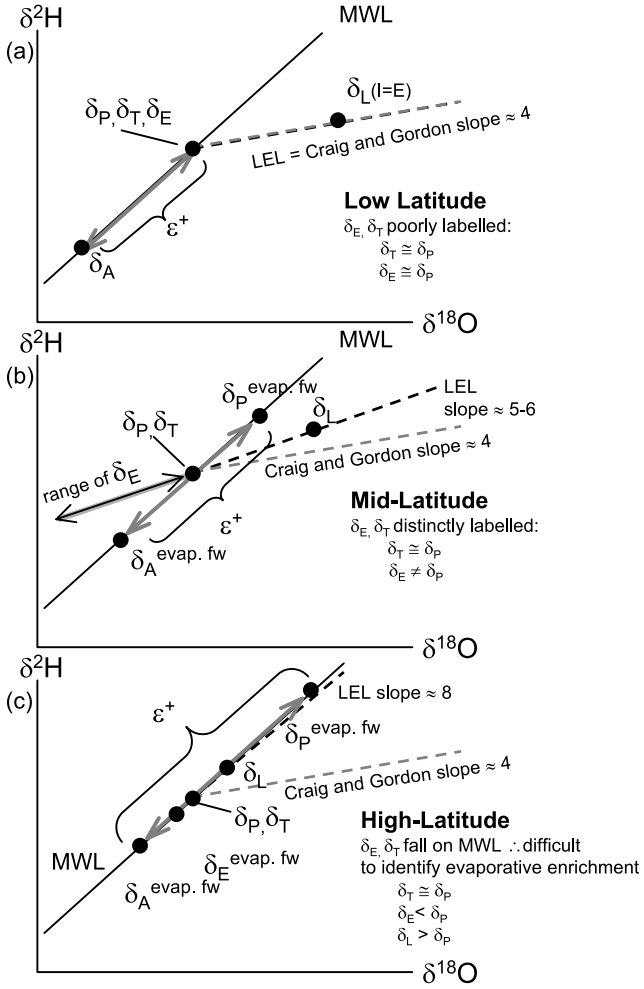

Figure 8. Conceptual model showing the effects of seasonality on the isotopic labeling of evaporation (δ_E) and transpiration (δ_T) and the potential for using isotopic labeling to distinguish between the two fluxes. At low latitudes (a), δ_E and δ_T will be poorly labeled as both will be very similar to the mean annual δ_P values. In midlatitude regions (b), there is a much better potential for isotopic labeling and separation of the evaporation and transpiration fluxes. At very high latitudes (c) the steepening of the LEL results in a situation where the evaporative flux will be indistinguishable isotopically from transpired moisture and precipitation because of the similarity of the MWL and LEL slopes. Note that ε^+ depicts the monthly flux-weighted value which is indistinguishable from the annual value for the idealized low-latitude scenario shown in Figure 8a.

[22] For high-latitude regions with highly seasonal climates our model suggests that the slopes of the LEL will at some point approach the slope of most MWLs (~8), creating a situation where the LEL is colinear with the MWL and δ_E, δ_T and δ_P all appear to plot on an apparent MWL. The similarity between the slopes of the LEL and MWL would make detecting evaporative enrichment effects and partitioning evaporation and transpiration more difficult, especially in the liquid phase. It is important to clarify that isotopic detection of evaporate and transpirate in the vapor phase should still be possible at extreme high latitudes as δ_E and δ_T are not expected to be identical. The tendency toward colinearity at high latitudes may however diminish the value of applying the dual tracer approach, although this remains to be verified.

References

Allison, G. B., and M. W. Hughes (1983), The use of natural tracers as indicators of soil-water movement in a temperate semi-arid region, *J. Hydrol.*, *60*, 157–173, doi:10.1016/0022-1694(83)90019-7.

Allison, G. B., C. J. Barnes, M. W. Hughes, and F. W. J. Leaney (1983), Effect of climate and vegetation on oxygen-18 and deuterium profiles in soils, in *Proceedings of the International Symposium on Isotope Hydrology in Water Resources Development*, *Rep. IAEA-SM-270/20*, pp. 105–123, Int. At. Energy Agency, Vienna.

Araguás-Araguás, L., K. Froehlich, and K. Rozanski (2000), Deuterium and oxygen-18 isotope composition of precipitation and atmospheric moisture, *Hydrol. Process.*, *14*(8), 1341–1355, doi:10.1002/1099-1085(20000615)14:8<1341::AID-HYP983>3.0.CO;2-Z.

Barnes, C. J., and G. B. Allison (1988), Tracing of water movement in the unsaturated zone using stable isotopes of hydrogen and oxygen, *J. Hydrol.*, *100*, 143–176, doi:10.1016/0022-1694(88)90184-9.

Birks, S. J., J. J. Gibson, L. Gourcy, P. K. Aggarwal, and T. W. D. Edwards (2002), Maps and animations offer new opportunities for studying the global water cycle, *Eos Trans. AGU*, *83*(37), 406.

Craig, H. (1961), Isotopic variations in meteoric waters, *Science*, *133*, 1702–1703, doi:10.1126/science.133.3465.1702.

Craig, H., and L. Gordon (1965), Deuterium and oxygen-18 in the ocean and the marine atmosphere, in *Stable Isotopes in Oceanographic Studies and Paleotemperatures*, edited by E. Tongiorgi, pp. 9–130, Spoleto, Italy.

Cressman, G. P. (1959), An operational objective analysis system, *Mon. Weather Rev.*, *87*, 367–374, doi:10.1175/1520-0493(1959)087<0367:AOOAS>2.0.CO;2.

Darling, W. G., and A. H. Bath (1988), A stable isotope study of recharge processes in the English chalk, *J. Hydrol.*, *101*, 31–46, doi:10.1016/0022-1694(88)90026-1.

Dinçer, T. (1968), The use of oxygen-18 and deuterium concentrations in the water balance of lakes, *Water Resour. Res.*, *4*, 1289–1305, doi:10.1029/WR004i006p01289.

Dinçer, T., W. Al-Mugrin, and V. Zimmermann (1974), Study of the infiltration and recharge through the sand dunes in arid zones with special reference to the stable isotopes and thermonuclear tritium, *J. Hydrol.*, *23*, 79–109, doi:10.1016/0022-1694(74)90025-0.

Fontes, J. C., and R. Gonfiantini (1967), Comportement isotopique au cours de l'evporation de deux bassins sahariens, *Earth Planet. Sci. Lett.*, *3*, 258–266, doi:10.1016/0012-821X(67)90046-5.

Fontes, J. C., F. Gasse, and E. Gibert (1996), Holocene environmental changes in Lake Bangong Basin (Western Tibet). part 1: Chronology and stable isotopes of carbonates of a Holocene lacustrine core, *Palaeogeogr. Palaeoclimatol. Palaeoecol.*, *120*, 25–47, doi:10.1016/0031-0182(95)00032-1.

Gat, J. R. (1995), Stable isotopes of fresh and saline lakes, in *Physics and Chemistry of Lakes*, edited by A. Lerman, D. Imboden, and J. R. Gat, pp. 139–165, Springer, Berlin.

Gat, J. R. (1996), Oxygen and hydrogen isotopes in the hydrologic cycle, *Annu. Rev. Earth Planet. Sci.*, *24*, 225–262, doi:10.1146/annurev.earth.24.1.225.

Gat, J. R. (2000), Atmospheric water balance: The isotopic perspective, *Hydrol. Process.*, *14*(8), 1357–1369, doi:10.1002/1099-1085(20000615)14:8<1357::AID-HYP986>3.0.CO;2-7.

Gat, J. R., and C. J. Bowser (1991), Heavy isotope enrichment in coupled evaporative systems, in *Stable Isotope Geochemistry: A Tribute to Samuel Epstein*, edited by H.P. Taylor et al., *Spec. Publ. Geochem. Soc.*, *3*, 159–168.

Gat, J. R., and E. Matsui (1991), Atmospheric water balance in the Amazon Basin: An isotopic evapotranspiration model, *J. Geophys. Res.*, *96*(D7), 13,179–13,188, doi:10.1029/91JD00054.

Gat, J. R., C. J. Bowser, and C. Kendall (1994), The contribution of evaporation from the Great Lakes to the continental atmosphere: Estimate based on stable isotope data, *Geophys. Res. Lett.*, *21*(7), 557–560, doi:10.1029/94GL00069.

Gibson, J. J. (2002), Short-term evaporation and water budget comparisons in shallow Arctic lakes using non-steady isotope mass balance, *J. Hydrol.*, *264*, 242–261, doi:10.1016/S0022-1694(02)00091-4.

Gibson, J. J., T. W. D. Edwards, G. G. Bursey, and T. D. Prowse (1993), Estimating evaporation using stable isotopes: Quantitative results and sensitivity analysis for two catchments in northern Canada, *Nordic Hydrol.*, *24*(2–3), 79–94.

Gibson, J. J., T. W. D. Edwards, S. J. Birks, N. A. St. Amour, W. M. Buhay, P. McEachern, B. B. Wolfe, and D. L. Peters (2005), Progress in isotope tracer hydrology in Canada, *Hydrol. Process.*, *19*, 303–327, doi:10.1002/hyp.5766.

Gonfiantini, R. (1986), Environmental isotopes in lake studies, in *Handbook of Environmental Isotope Geochemistry*, edited by P. Fritz and J. C. Fontes, pp. 113–168, Elsevier, New York.

Hamilton, S. K., S. E. Bunn, M. C. Thoms, and J. C. Marshall (2005), Persistence of aquatic refugia between flow pulses in a dryland river system, *Limnol. Oceanogr.*, *50*(3), 743–754.

Hammarlund, D., S. Bjorck, B. Buchardt, C. Israelson, and C. T. Thomsen (2003), Rapid hydrological changes during the Holocene revealed by stable isotope records of lacustrine carbonates from Lake Igelsjon, southern Sweden, *Quat. Sci. Rev.*, *22*, 353–379, doi:10.1016/S0277-3791(02)00091-4.

Horita, J., and D. Wesolowski (1994), Liquid-vapour fractionation of oxygen and hydrogen isotopes of water from the freezing to the critical temperature, *Geochim. Cosmochim. Acta*, *58*, 3425–3437, doi:10.1016/0016-7037(94)90096-5.

Kalnay, E., et al. (1996), The NCEP/NCAR 40-year reanalysis project, *Bull. Am. Meteorol. Soc.*, *77*, 437–471, doi:10.1175/1520-0477(1996)077<0437:TNYRP>2.0.CO;2.

Kurita, N., N. Yoshida, G. Inoue, and E. A. Chayanova (2004), Modern isotope climatology of Russia: A first assessment, *J. Geophys. Res.*, *109*, D03102, doi:10.1029/2003JD003404.

Leng, M. J., and N. J. Anderson (2003), Isotopic variation in modern lake waters from western Greenland, *Holocene*, *13*(4), 605–611, doi:10.1191/0959683603hl620rr.

Maulé, C., D. S. Chanasyk, and K. Muehlenbachs (1994), Isotopic determination of snow-water contribution to soil water and groundwater, *J. Hydrol.*, *155*, 73–91, doi:10.1016/0022-1694(94)90159-7.

Merlivat, L. (1978), Molecular diffusivities of $H_2^{16}O$, $HD^{16}O$, and $H_2^{18}O$ in gases, *J. Chem. Phys.*, *69*(6), 2864–2871, doi:10.1063/1.436884.

New, M., M. Hulme, and P. Jones (1999), Representing twentieth-century space-time climate variability. part I: Development of a 1961–90 mean monthly terrestrial climatology, *J. Clim.*, *12*(3), 829–856, doi:10.1175/1520-0442(1999)012<0829:RTCSTC>2.0.CO;2.

Rietti-Shati, M., R. Yam, W. Karlen, and A. Shemesh (2000), Stable isotope composition of tropical high-altitude fresh-waters on Mt. Kenya, equatorial East Africa, *Chem. Geol.*, *166*, 341–350, doi:10.1016/S0009-2541(99)00233-8.

Rozanski, K., K. Froehlich, and W. G. Mook (2001), Surface water, in *Environmental Isotopes in the Hydrological Cycle: Principles and Applications*, edited by W. G. Mook, 117 pp., UNESCO, Paris.

Stewart, C. L. (1994), An isotopic investigation of passive dewatering of tailings at the Lupin Mine site, Northwest Territories, B.Sc. thesis, Univ. of Waterloo, Ontario, Canada.

Teranes, J. L., and J. A. McKenzie (2001), Lacustrine oxygen isotope record of 20th-century climate change in central Europe: Evaluation of climatic controls on oxygen isotopes in precipitation, *J. Paleolimnol.*, *26*(2), 131–146, doi:10.1023/A:1011175701502.

Turner, J. V., G. B. Allison, and J. W. Holmes (1984), The water balance of a small lake using stable isotopes and tritium, *J. Hydrol.*, *70*, 199–220, doi:10.1016/0022-1694(84)90122-7.

Vogt, H. J. (1976), *Isotopentrennung bei der Verdampfung von Wasser*, 78 pp., Univ. of Heidelberg, Germany.

von Grafenstein, U. (2002), Oxygen-isotope studies of ostracods from deep lakes, in *The Ostracoda: Applications in Quaternary Research*, *Geophys. Monogr. Ser.*, vol. 131, edited by J. A. Holmes and A. R. Chivas, pp. 249–266, AGU, Washington, D. C.

Wolfe, B. B., and T. W. D. Edwards (1997), Hydrologic control on the oxygen-isotope relation between sediment cellulose and lake water, western Taimyr Peninsula, Russia: Implications for the use of surface-sediment calibrations in paleolimnology, *J. Paleolimnol.*, *18*(3), 283–291, doi:10.1023/A:1007997422237.

Wolfe, B. B., T. W. D. Edwards, K. R. M. Beuning, and R. J. Elgood (2001), Carbon and oxygen isotope analysis of lake sediment cellulose: Methods and applications, in *Tracking Environmental Change Using Lake Sediments: Physical and Chemical Techniques, Developments in Paleoenvironmental Research*, edited by W. M. Last and J. P. Smol, pp. 373–400, Kluwer Acad. Publ., Dordrecht, Netherlands.

Yang, W., R. J. Spencer, H. R. Krouse, T. K. Lowenstein, and E. Casas (1995), Stable isotopes of lake and fluid inclusion brines, Dabusun Lake, Qaidam Basin, western China: Hydrology and paleoclimatology in arid environments, *Palaeogeogr. Palaeoclimatol. Palaeoecol.*, *117*, 279–290, doi:10.1016/0031-0182(94)00126-S.

Yehdegho, B., K. Rozanski, H. Zojer, and W. Stichler (1997), Interaction of dredging lakes with the adjacent groundwater field; an isotope study, *J. Hydrol.*, *192*(1–4), 247–270, doi:10.1016/S0022-1694(96)03102-2.

Zuber, A. (1983), On the environmental isotope method for determining the water balance components of some lakes, *J. Hydrol.*, *61*, 409–427.

S. J. Birks, Alberta Research Council, 3608-33 Street NW, Calgary, Alberta, T2L 2A6, Canada.

T. W. D. Edwards, Department of Earth and Environmental Sciences, University of Waterloo, Waterloo, Ontario, Canada.

J. J. Gibson, Alberta Research Council, c/o Department of Geography, University of Victoria, P.O. Box 3060, STN CSC, Victoria, BC, V8W 3R4, Canada. (jjgibson@uvic.ca)